2584–2595 *Nucleic Acids Research, 2007, Vol. 35, No. 8* *Published online 4 April 2007*
doi:10.1093/nar/gkm186

Base-flipping dynamics in a DNA hairpin processing reaction

Julien Bischerour and Ronald Chalmers*

University of Oxford, Department of Biochemistry, South Parks Road, Oxford, OX1 3QU, UK

Received February 13, 2007; Revised March 14, 2007; Accepted March 15, 2007

ABSTRACT

Many enzymes that repair or modify bases in double-stranded DNA gain access to their substrates by base flipping. Although crystal structures provide stunning snap shots, biochemical approaches addressing the dynamics have proven difficult, particularly in complicated multi-step reactions. Here, we use protein–DNA crosslinking and potassium permanganate reactivity to explore the base-flipping step in Tn*5* transposition. We present a model to suggest that base flipping is driven by a combination of factors including DNA bending and the intrusion of a probe residue. The forces are postulated to act early in the reaction to create a state of tension, relieved by base flipping after cleavage of the first strand of DNA at the transposon end. Elimination of the probe residue retards the kinetics of nicking and reduces base flipping by 50%. Unexpectedly, the probe residue is even more important during the hairpin resolution step. Overall, base flipping is pivotal to the hairpin processing reaction because it performs two opposite but closely related functions. On one hand it disrupts the double helix, providing the necessary strand separation and steric freedom. While on the other, transposase appears to position the second DNA strand in the active site for cleavage using the flipped base as a handle.

INTRODUCTION

Base flipping is a type of DNA distortion in which an individual base is rotated into an extra-helical location. This term was coined for the DNA methylases in which a single nucleoside is rotated through ~180° into an extra-helical location (1,2). However, the term has come to be used colloquially and is often applied to systems that rotate the entire nucleotide, including a backbone phosphate. The most obvious reason that an enzyme would employ this mechanism is to gain access to a base that would otherwise remain inaccessible, buried in the double helix. There are many clear examples of this type such as the DNA methylases and glucosyltransferases that modify DNA, and the DNA glycosylases that remove damaged and mismatched bases (3–7).

There is also evidence for base flipping in other processes where the utility of the mechanism is less obvious. The most important examples are the initiation of transcription, protein translation in the ribosome and DNA replication (8–12). These are complicated reactions, which are perhaps more difficult to study than the methylases and glycosylases where the base-flipping step yields the foremost intermediate. In this article, we explore the dynamics of base flipping in another complicated, multistep reaction, namely DNA transposition. Tn*5* is a member of the IS*4* family of elements that includes the other well-characterized element Tn*10* and contributes to the spread of antibiotic resistance in bacteria (13–15,16: and references therein). Members of this family transpose by a 'cut-and-paste' mechanism in which the element is excised from the donor site by double-strand breaks at both ends of the element, followed by integration at a target site. In principle, cut-and-paste transposition can be achieved without recourse to a base-flipping step. However, the cocrystal structure of the Tn*5* post-cleavage intermediate shows that the penultimate nucleoside on the 'top strand' of the transposon is flipped into a 'stabilization pocket' in the protein (17). This aspect of the structure was unexpected because the flipped thymine is not subject to any kind of modification such as methylation or excision.

One explanation for the base-flipping step in Tn*5* is that it is part of a curious solution to the mechanistic problem of cleaving both strands of DNA at the transposon end. One monomer of transposase can bind sequence-specifically to the transposon end where it is positioned to nick one of the DNA strands. The problem arises because the sequences flanking the transposon are variable and there are therefore no sequence-specific interactions available to locate a second monomer in a symmetrical position to nick the second strand. The solution adopted by the IS*4* family of elements is to use a single monomer of transposase together with a

*To whom correspondence should be addressed. Tel: 44 1865 275307; Fax: 44 1865 275297

DNA-hairpin intermediate (18,19) (Figure 1). The first step of the reaction is a simple nick that generates the 3'-OH at the end of the transposon. The double-strand break is then achieved when the 3'-OH is used to attack the second strand in a direct transesterification reaction that generates the hairpin intermediate. The reaction is completed by a simple resolution of the hairpin structure on the transposon end.

Two different mechanisms for the hairpin reaction have evolved within the DDE family of elements. In the eukaryotic *hAT* family, the polarity of the hairpin reaction is completely reversed compared to the bacterial elements such as Tn*5* (20) (Figure 1). Because the first nick generates the 5'-phosphate at the end of the transposon, subsequent steps yield a hairpin on the flanking DNA, rather than the transposon end. This variation has proven to be extremely significant because it is used in the vertebrate immune system where it provides the mechanism by which antibody and T cell receptor diversity is generated (21). In light of its close relationship to transposition, it is likely that V(D)J recombination will also employ a base-flipping mechanism (22,23). It will be interesting to discover how reversal of the reaction polarity is accommodated.

In the present work, we propose a model to suggest that base flipping in Tn*5* is driven by a combination of DNA binding, bending and the intrusion of a probe residue into the DNA helix. Although these forces act at an early stage, the target base is denied access to the stabilization pocket until after the first nick. Base flipping is associated with a distortion of the DNA helix extending in the 5'-direction. Presumably this facilitates the hairpin formation step which requires separation of the strands. The function of the probe residue becomes even more important during the hairpin resolution step. Most likely it is required to act as a 'doorstop' once the disrupting influence of the DNA bend is unavoidably lost owing to the double-strand break. Although some elements of the Tn*5* base-flipping reaction have precedents in other systems, they have been observed here working together in a single dynamic reaction.

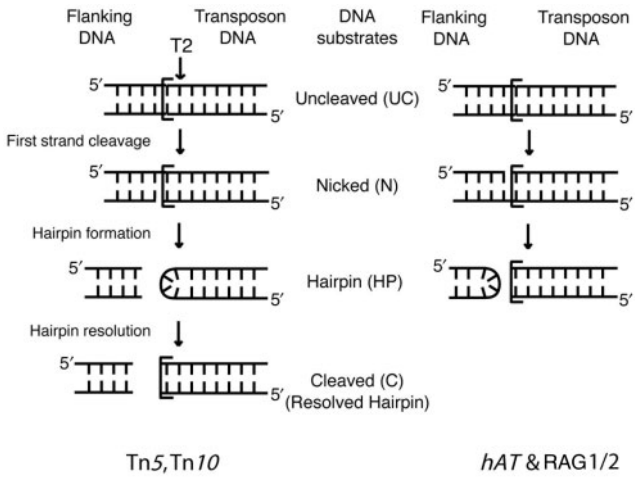

Figure 1. Two hairpin processing reactions of opposite polarity. In Tn*5* and Tn*10*, the first step of the cleavage reaction is a nick that generates the 3'-OH at the end of the transposon. This group is used in a direct transesterification reaction to cleave the opposite strand, generating a hairpin intermediate on the transposon end. Resolution by nick at the tip of the hairpin yields a blunt transposon end. In V(D)J recombination and the *hAT* family of eukaryotic transposons, the polarity of the reaction is reversed and the first nick generates the 5'-P at the end of the transposon. The subsequent transesterification reaction yields a blunt-ended transposon and a hairpin on the flanking DNA. The flanking hairpin is processed by the host during double-strand break repair. Imprecise rejoining of the hairpin ends generated by the RAG1–2 complex in V(D)J recombination produces the sequence variations that underlie T cell receptor and antibody diversity. Open rectangular boxes represent transposon ends and/or the V(D)J recombination signal sequences.

RESULTS

The flipped base stacks on the W298 residue after the first nick

In the cocrystal structure of the post-cleavage Tn*5* transpososome, the thymidine at position 2 of the non-transferred strand (T2) is flipped out of the DNA helix and stacked against the indol ring of tryptophan W298 (Figure 2A). To probe this interaction, we substituted the T2 residue with the zero-length crosslinking agent 5-iodouracil (IdU). This modification does not affect the activity of the transposase (not shown). Tn*5* transpososomes were assembled with uncleaved (UC), nicked (N) and cleaved (C) IdU-substrates. The complexes were irradiated with UV to induce crosslinking, and analyzed by SDS-PAGE (Figure 2B).

In the presence of the standard transposase, two crosslinked products were detected (Figure 2B, lanes 4–6). Although both products appear to be specific, we were unable to identify the source of this heterogeneity. No crosslinked products were detected in the absence of the IdU base (not shown), UV exposure (not shown) or in the absence of transposase (Figure 2B, lanes 1–3). The efficiency of crosslinking increased substantially with substrates mimicking later step of the reaction (Figure 2C). There is a 5-fold increase after the first nick and a further 1.4-fold increase after second strand cleavage.

When the complexes were assembled with the W298A transposase, crosslinking was reduced almost to the level of the background in the gel (Figure 2B, lanes 7–9). The remaining signal does not appear to be specific as it does not increase with the substrates that mimic later stages of the reaction. Instead, the signal for the cleaved complex is less than in the uncleaved and nicked complexes (compare lanes 7–9). To rule out any indirect effects of the W298A mutation, the identity of the crosslinked amino acid residue was determined directly by protein sequencing. The complex was assembled with the cleaved IdU substrate, exposed to UV and digested with trypsin. The DNA adducts were then purified from free DNA and non-crosslinked peptides by cation exchange chromatography. The crosslinked peptides were sequenced by automated Edman degradation.

Two overlapping peptide sequences were obtained, starting immediately after the trypsin cleavage sites at lysine 273 and 291 of the Tn*5* transposase (Figure 2D).

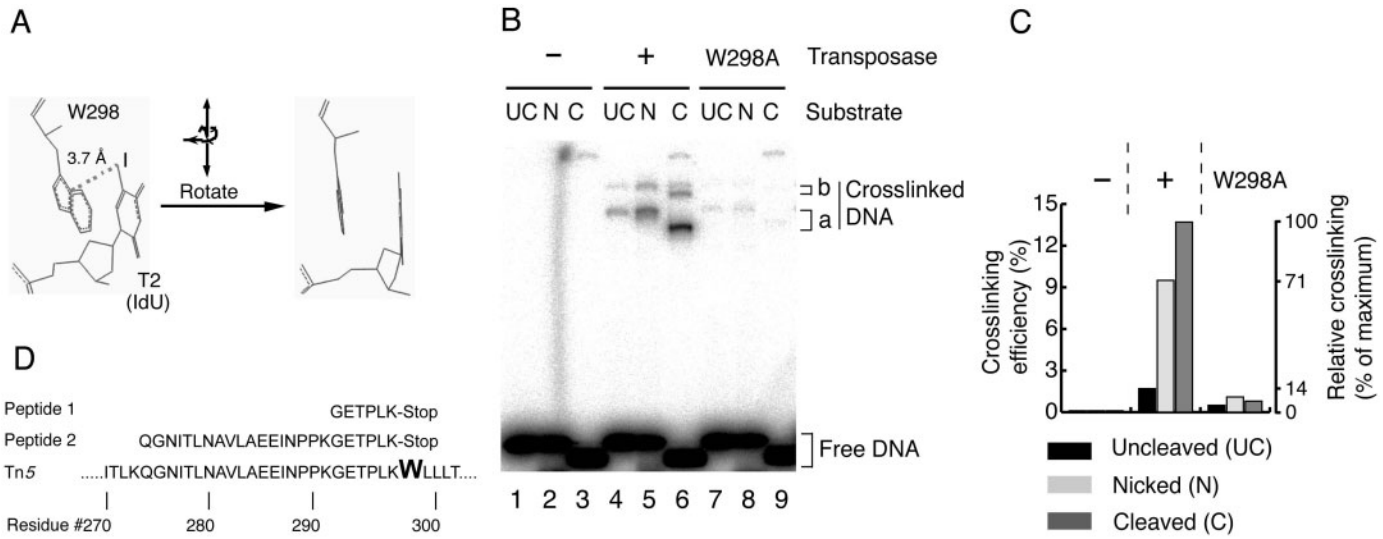

Figure 2. Base flipping increases as the reaction progresses. (**A**) The spatial relationship between the W298 residue and the flipped base at position T2. The coordinates are taken from the post-cleavage cocrystal structure for Tn*5* (17). The crosslinking substrates were generated by replacing the 5-methyl group of the thymine with iodine (iodouracil). (**B**) The crosslinking assay was performed with uncleaved, nicked and cleaved substrates that mimic the progression of the cleavage reaction. Two specific crosslinked products were detected. Note that the products with the cleaved substrate migrate faster because the DNA adducts lack flanking sequences and are therefore shorter. Crosslinking is abolished when W298 is substituted with alanine. The DNA was 3'-end labeled with ^{32}P. An autoradiogram of an SDS-PAGE is shown. (**C**) The crosslinked products were quantified using a phosphorimager. Crosslinking efficiency is given as the percentage of total radioactivity present in the crosslinked products. To normalize the reactions for potential differences in the amount of DNA incorporated into the complexes, an aliquot of each reaction was removed immediately before exposure to UV light and analyzed using the standard EMSA. In practice, very little variation was present, as the amount of bound DNA was usually close to 100%. Normalization of the crosslinking was achieved by dividing the crosslinking signal by the fraction of DNA bound in the EMSA. The results show that there is a 5-fold increase in crosslinking after the first nick and a further 1.4-fold increase after second strand cleavage. (**D**) After crosslinking, the cleaved complex was treated with trypsin. The DNA–peptide adducts were purified from free DNA and non-crosslinked peptides and sequenced by automated Edman degradation. Two sequences were obtained starting immediately after trypsin cleavage sites and ending immediately before W298. The recovery of two sequences reflects incomplete trypsin digestion at the K residue closest to the site of crosslinking.

Both peptide sequences terminated immediately before the expected crosslinking site at W298. The same result was obtained in two further independent experiments. Together with the experiments above, this result confirms that the crosslinking signal is indicative of stacking between the T2 base and W298.

The key result of the crosslinking experiment is that base flipping increases as the reaction progresses (Figure 2B and C). The large increase in base flipping after the first nick suggests that it is required for the following step when strand separation is required for processing the DNA hairpin intermediate.

Destabilization of the DNA helix before the first nick

To explore any structural changes preceding the first nick, we designed a positive display assay to probe the structure of the DNA helix in the immediate vicinity of the transposon end. Potassium permanganate ($KMnO_4$) reacts with thymine bases in distorted DNA, particularly if they are in an extra-helical position (24,25). Tn*5* transpososomes were assembled with uncleaved or nicked substrates, and treated with $KMnO_4$ (Figure 3). For this assay, we used a transposon end with a T residue placed at position −1 in the flanking DNA (T-1). The assay can therefore report on the chemical environment of the bases on either side of the terminal C residue that is subjected to nucleophilic attack by the 3'-OH during the hairpin step of the reaction. In the presence of transposase, T2 and T − 1 are the only thymines that display a significant increase in $KMnO_4$ sensitivity (Figure 3, compare lanes 1 and 2). Unexpectedly, T − 1 was more sensitive than T2. Furthermore, T − 1 sensitivity increased dramatically after the first nick, suggesting a progressive disruption of the DNA helix. However, contrary to the expectation from the crosslinking experiment, the sensitivity of T2 was unaffected by the nick, and remains less than what might be expected if the base was flipped out of the helix (25).

The W298A mutation reveals base flipping in the uncleaved transpososome

One explanation for the unexpectedly low $KMnO_4$ sensitivity of T2 in the nicked transpososome is that the base is protected, either by its location within a pocket, or by specific stacking against W298. To test this hypothesis, the W298A mutant was assayed for $KMnO_4$ sensitivity (Figure 4A).

The W298A mutation produced a 10-fold increase in $KMnO_4$ sensitivity at T2 (Figure 4A, compare lanes 2 with 3, and 7 with 8). The signal at T2 was therefore 5-fold greater than that at T − 1, which is more consistent with a flipped state of T2 in the cocrystal structure. The enhanced signal was present with the uncleaved and the nicked substrates, suggesting that T2 is flipped before first strand nicking in this mutant. Taken together, these results confirm that W298 protects the flipped T2 base

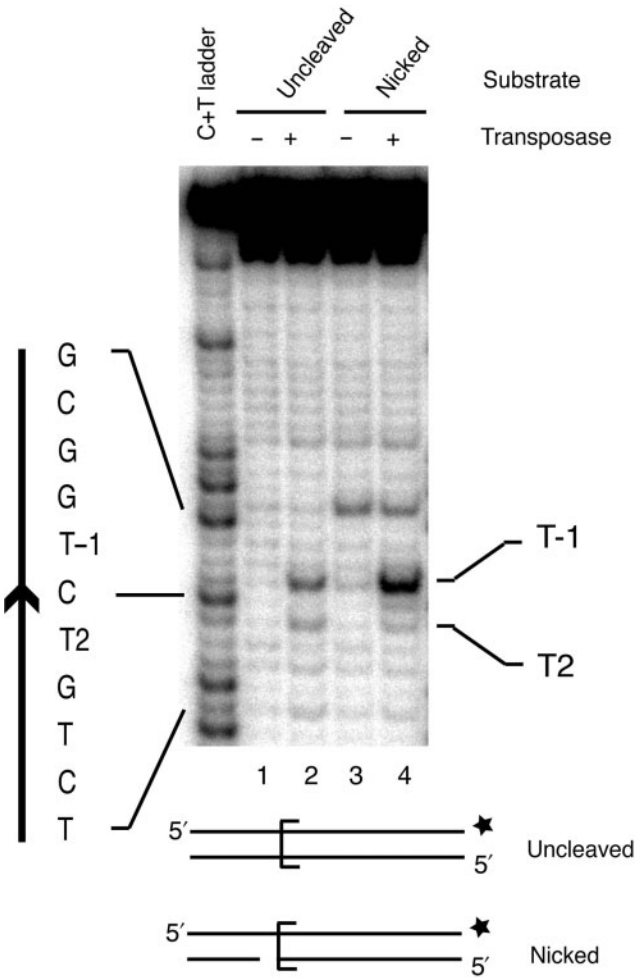

Figure 3. Permanganate sensitivity at the transposon end. Complexes were assembled with uncleaved or nicked substrate and treated with $KMnO_4$. $KMnO_4$ oxidizes thymine bases in distorted DNA, particularly if they are in an extra-helical position (25). Oxidation converts the thymine to *cis*-thymine glycol which, upon piperidine treatment, undergoes further degradation leading to cleavage of the DNA strand. Following treatment, the DNA was recovered and the pattern of sensitivity displayed on a DNA sequencing gel. The arrowhead indicates the location of the transposon end. The substrates were 3'-end labeled as indicated by the asterisk.

from $KMnO_4$ in the nicked complex. They also show that base flipping is not driven by stabilizing interactions between T2 and W298, as would be expected in a passive-capture mechanism for base flipping. On the contrary, the W298A mutation seems to allow base flipping to occur in the uncleaved complex, one step earlier than normal.

The W323 residue helps to drive base flipping

The results presented above suggest that base flipping is driven by residues other than W298. Inspection of the post-cleavage crystal structure reveals a good candidate: a second tryptophan at position 323 penetrates the minor groove of the DNA opposite the position of T2 (Figure 4B). It is tempting to suggest that this residue acts at earlier stages of the reaction as a probe to extrude the T2 base from the helix. The W323 residue is located immediately after the arginine residue in the catalytically important YREK motif. This position is equivalent to the Tn*10* M289I mutation which is defective for hairpin formation (26).

If W323 drives base flipping, substitution with the shorter side chain of an alanine residue should reduce $KMnO_4$ sensitivity at T2. This was confirmed, but the difference was difficult to quantify because of the initially low signal with the standard protein (Figure 4A, compare lane 2 with 4, and lane 7 with 9). This problem was circumvented by taking advantage of the increased signal in the W298A background. In the double mutant, T2 sensitivity in the uncleaved and nicked substrates was reduced by 50 and 65%, respectively (compare lane 3 with 5, and lane 8 with 10).

The catalytic effects of W323A and W298A mutations

To further investigate the effects of the W323A mutation, we determined the kinetics of the cleavage reaction (Figure 5). The substrate was radiolabeled on both 3'-ends so that the nick, hairpin and resolved product could all be detected and quantified in a single experiment.

In the control reaction with an uncleaved substrate, the first nick is detected after 2 min. However, in W323A the first nick is delayed and none is detected before the 15-min time point (Figure 5A). The hairpin intermediate also accumulates owing to a clear defect in resolution. To determine whether hairpin formation is also affected, the experiment was repeated with a pre-nicked substrate (Figure 5B). The early time points in the W323A reaction were very similar to the control and hairpin was detected after 2 min. These results support the importance of the W323 residue for the nicking step of the reaction, as was inferred from the 50% reduction in base flipping in the uncleaved substrate (Figure 4). They also emphasize that other factors in addition to the probe residue contribute to base flipping. Overall, the present results show that the W323A mutation delays the first nick, has little effect on hairpin formation, but is unexpectedly deleterious for hairpin resolution.

W298 mutations were previously shown to be defective in hairpin formation (27). However, kinetic analysis revealed a further subtle defect in the nicking step compared to the control (Figure 5C). The W298A reaction was similar to the control at the earliest time points, but after 10 min the rate decreased by ~50%. A similar effect has been observed in Tn*10* under conditions that also block hairpin formation (28). Although a precise explanation remains elusive, the effect probably stems from an allosteric coupling between opposite sides of the complex (29). In Tn*10*, this is reflected by the accumulation of the single-end break intermediate in which only one of the two transposon ends has been cleaved. However, we have not yet confirmed whether the W298 mutation in Tn*5* also produces this effect.

The partial activities of the W298 and W323 mutations show that these residues operate together with other factors to promote the progressive conformational changes required for the reaction. More distantly located

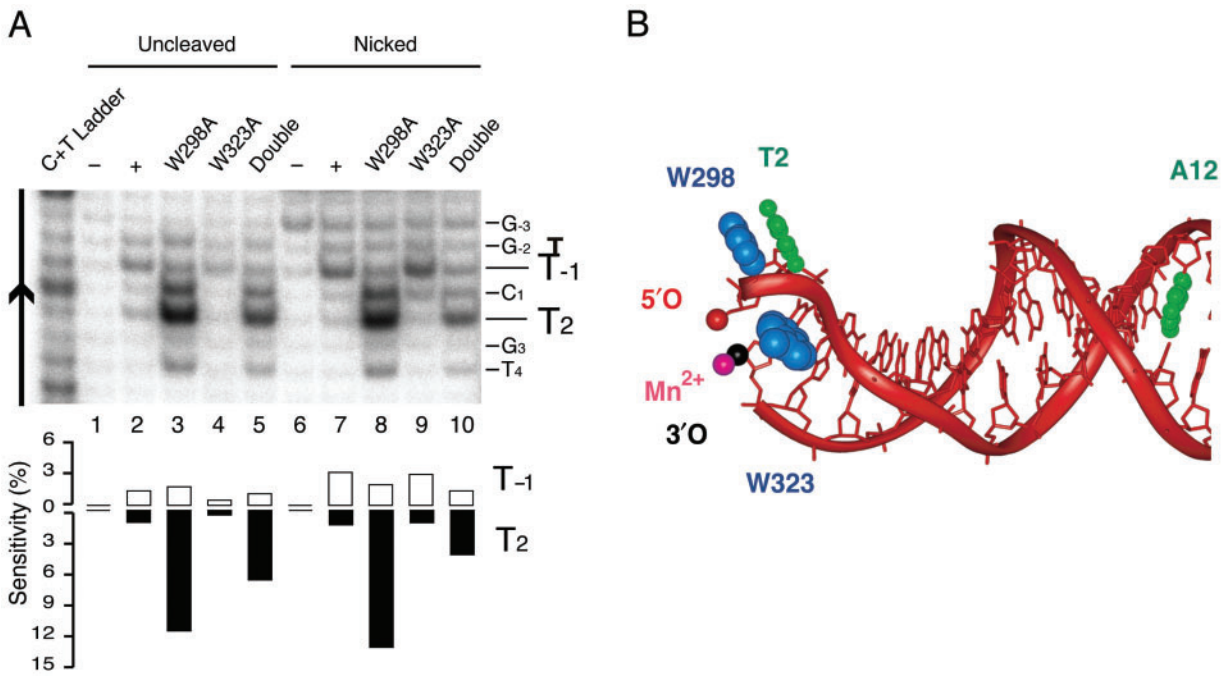

Figure 4. Mutations in the probe and stacking residues affect base flipping in opposite directions (**A**) Complexes were assembled with the indicated transposase mutants as described in Figure 3. The bands were quantified using a phosphorimager as indicated below the gel. The sensitivity at each position is expressed as a percentage of the total DNA present in the transpososome complex. To normalize the reactions for potential differences in the amount of DNA incorporated into the complexes, an aliquot of each reaction was removed immediately before $KMnO_4$ treatment and analyzed using the standard EMSA. In practice, very little variation was present. Normalization was achieved by dividing the phosphorimager signal by the fraction of the total DNA bound by transposase in the EMSA. (**B**) One of the transposon ends from the Tn*5* cocrystal structure is shown together with two key tryptophan residues. The other transposon end and the rest of the protein are omitted for clarity. W323 is inserted into the DNA helix and appears to act either as a probe to extrude the T2 base, or to prevent its return by occupying the vacated space. T2 is stacked against W298.

DNA–protein interactions with the transposon arm and the flanking DNA are likely additional contributors. Hence, the reaction is able to tolerate single perturbations.

The W323A mutant reveals an early reaction intermediate

The ability of the W323A transposase to assemble the transpososome complex with uncleaved and nicked substrates was tested using an electrophoretic mobility shift assay (EMSA, Figure 6A). The total amount of complex formed was equivalent to the control. However, the complex migrated more slowly. Henceforth, we will refer to the different complexes as 'slow' or 'fast'. There are two lines of evidence to suggest that the slow complex is an alternative form of the synaptic complex. First, in the EMSA, the complex between transposase and a single transposon end has been shown to migrate much faster than the synaptic complex (30). Second, the EMSA failed to resolve two complexes in experiments with 40 bp substrates having 20-bp transposon arms and 20-bp flanking DNA (not shown). The dependence of the slow complex on the 90-bp substrates used here suggests that it may represent change in the relative position of the flanking DNA and the transposon arm.

The slow migration of the W323A complex was largely rescued by using the nicked substrate (Figure 6A, lane 9). We interpret this result as showing that W323A has a DNA-bending defect. First, the transpososome is essentially a four-way junction between the two transposon arms and the flanking DNA. The gel-mobility of the complex is therefore extremely sensitive to the conformation of the DNA. A bend in the DNA may therefore result in faster migration due to compaction of the structure, as has been documented in Tn*10* (31,32). Second, the slow migration of the W323A complex is rescued by the nick at bp + 1 in the nicked substrate. The nick is likely to increase the flexibility of the DNA and facilitate the transposase-induced bend that has been detected at bp + 2 using circular permutation and bend-phasing techniques (33). These considerations suggest that the slow-migrating W323A complex represents an early intermediate of the reaction in which the DNA component is possibly in an extended, unbent conformation. This is probably a natural feature of the reaction as trace levels are detected in the standard and W298A reactions (Figure 6A, lanes 2 and 3).

The slow migration of the W323A complex was also largely rescued in a W298A background (Figure 6, lane 5). This fits with the $KMnO_4$ results which showed that W298 presents a resistance to base flipping in the uncleaved complex (above, Figure 4). Taken together, these observations provide a link between DNA bending, insertion of the W323 probe residue and base flipping.

To investigate these issues further, we searched for reaction conditions that would favor the assembly of the slow complex. The standard reaction buffer, used in all of the experiments described so far, contained 5 mM $CaCl_2$. We found that replacing the $CaCl_2$ with EDTA

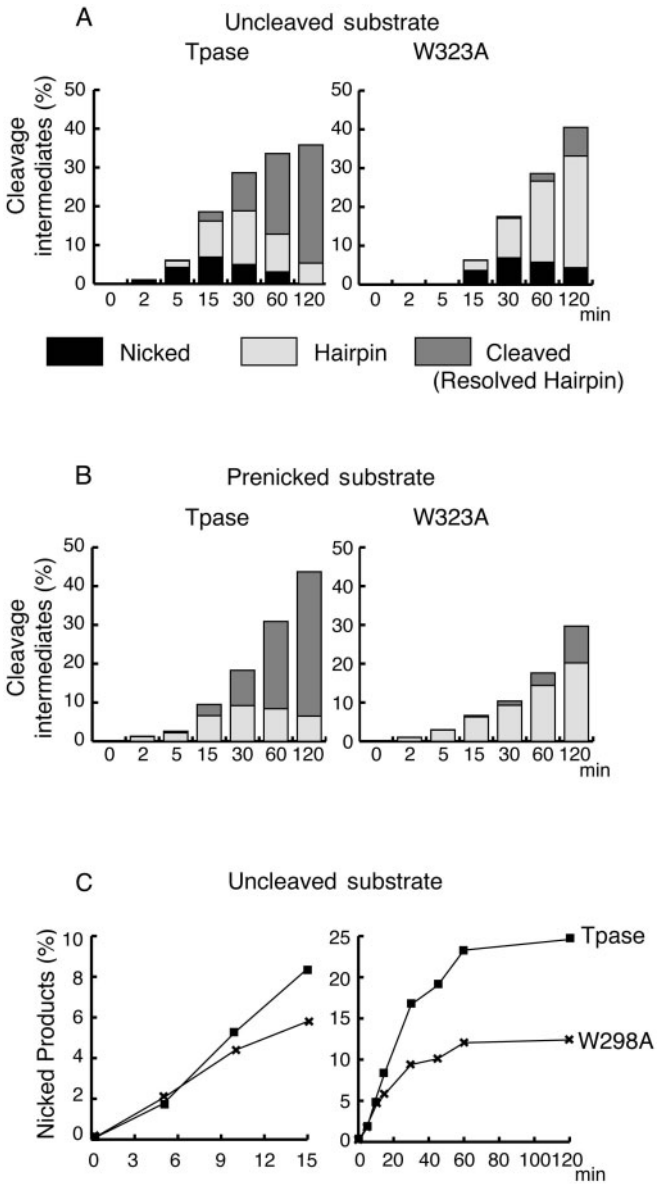

Figure 5. The catalytic defects arising from mutations in the probe and stacking residues (**A** and **B**). Transposition reactions were performed with uncleaved and nicked substrates as indicated. The complexes were assembled in the standard buffer and the reactions were initiated by the addition of 5 mM $MgCl_2$. Aliquots were removed at the indicated times and treated with EDTA and SDS to stop the reaction. The substrate was labeled on both 3'-ends so that nicks, hairpin and the cleaved transposon end could be detected simultaneously by analysis on a DNA sequencing gel. The products were quantified using a phosphorimager. In this labeling strategy, the nicked intermediate is revealed by the presence of the bottom-cleaved strand of the flanking DNA (see illustration in Figure 1). This is an end product of the reaction and accumulates throughout. The amount of the nicked intermediate at each time point is therefore obtained by subtracting the sum of the unique fragments produced by hairpin formation and resolution. The results are expressed as a percentage of the total DNA present in the reaction. Since all of the complexes that form initially go on to complete the reaction, the maximum height of the histogram at the last time point indicates the fraction of DNA bound in complexes at the start of the reaction. (**C**) Transposition reactions were performed with the W298A transposase as just described using the uncleaved substrate. The results are plotted twice with different scales to clearly illustrate the difference between the behavior of the transposase and the W298A mutant at early and late time points.

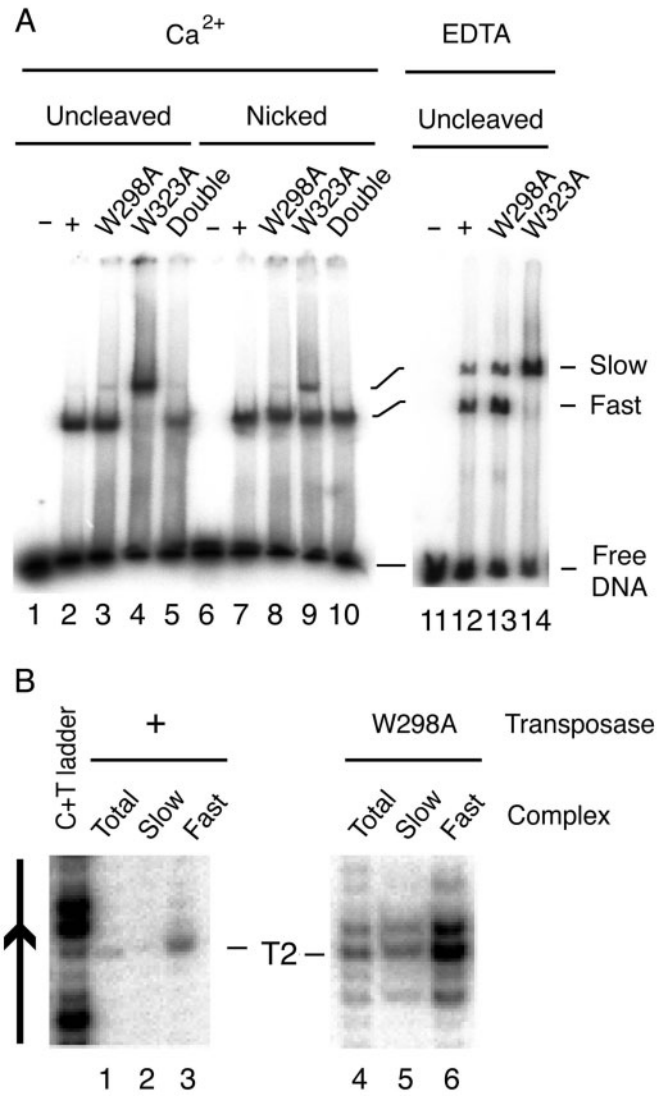

Figure 6. Base flipping is associated with DNA bending. (**A**) Transpososome complexes were assembled with the uncleaved or pre-nicked substrate under standard conditions in the presence of Ca^{++} or EDTA. The complexes were visualized using the standard EMSA, followed by autoradiography. With the uncleaved substrate, the W323A mutant yields a complex that migrates slowly. Trace amounts of this complex are also detected with the standard and the W298A mutant transposases. (**B**) The slow and fast complexes in part A were located by autoradiography and excised from the gel. The $KMnO_4$ reaction was performed in the gel slice. The complexes were disrupted by SDS treatment and the DNA was recovered by the crush and soak method. The pattern of $KMnO_4$ sensitivity was displayed on a DNA sequencing gel. Lanes 1 and 4 show the $KMnO_4$ sensitivity of the 'total' complexes present in an aliquot of the respective reactions before separation in the EMSA. The reactions were normalized by loading the same amount of DNA in each lane, determined by radioactive counting.

significantly increased the amount of slow complex with W298A and the control (Figure 6, lanes 12 and 13). The complete removal of divalent metal ions can potentially affect the complex in at least two ways. The DNA will be generally stiffer because of a reduction in charge shielding in the phosphodiester backbone. Furthermore, there may

be a specific effect stemming from the absence of Ca^{++} which serves as a non-catalytic analog of the Mg^{++} that would normally occupy the active site. In either case, it seems likely that the retardation of the slow complex is the result of a change in the conformation of the DNA which is presumably in a more extended, less bent, conformation.

The slow complex precedes base flipping in the reaction

The $KMnO_4$ assay was used to probe the relationship between base flipping and the slow and fast forms of the complex. Uncleaved complexes were assembled with 5 mM EDTA in the binding buffer. An aliquot was treated with $KMnO_4$ directly to provide the 'total' or average signal (Figure 6B). The fast and slow complexes in the remainder of the solution were separated in the standard EMSA, located by autoradiography and excised from the gel. The $KMnO_4$ reaction was then performed in the gel slice and the products were recovered by the crush and soak method. The reactions were normalized for variations in the recovery of the DNA by loading the same number of radioactive counts on each lane of the sequencing gel used for analysis.

With the standard transposase protein, most of the $KMnO_4$ sensitivity at T2 was derived from the fast complex (Figure 6B, lanes 1–3). The difference was difficult to quantify because of the low starting signal. However, when the W298A mutant was used to increase the $KMnO_4$ signal at T2, the reactivity was 5-fold lower in the slow complex suggesting that the base is not yet flipped. The slow complex therefore appears to represent a reaction intermediate that precedes base flipping.

DISCUSSION

A model for base flipping dynamics during DNA hairpin processing

The results presented here are summarized in a model for Tn*5* base-flipping dynamics (Figure 7). The model illustrates the structural intermediates detected during the cleavage steps of the reaction. In lines 3–5 of the model, the 3D position of T2 relative to the two tryptophan residues is provided by cocrystal structure of the transpososome (Figure 4B). In lines 1 and 2, the T2 base and W323 have been moved to illustrate the dynamics of the reaction revealed by the biochemical experiments. The evidence supporting each of the structures, and the roles of the W298 and W323 residues are given as follows:

Complex 1. The 'uncleaved slow' complex is proposed to be an early intermediate of the reaction in which the DNA is in an extended, unbent configuration. Only trace amounts are detected with the standard transposase protein, but significant enrichment is achieved when the complex, is assembled in EDTA or in the W323A background (Figure 6A). In this complex the bases surrounding the transposon end are not sensitive to $KMnO_4$, even in the W298A background, indicating that they remain stacked within the DNA helix (Figure 6B).

Complex 2. The 'uncleaved fast' complex is the major species produced by the standard transposase (Figure 6A). This complex immediately precedes the first catalytic step of the reaction and appears to be poised in a state of tension. The forces that disrupt the DNA helix in preparation for the hairpin step are already acting, but they are opposed by the presence of W298.

In complex 2, the most prominent $KMnO_4$ signal is at position $T-1$ in the flanking DNA (Figure 4A, lane 2). This suggests that although the DNA helix is distorted, it remains largely intact. This is consistent with the low IdU crosslinking signal which shows that T2 is not yet stacked against W298 (Figure 2, lane 4).

The $KMnO_4$ sensitivity of complex 2 is markedly reduced by the W323A mutation (Figure 4A, lanes 4 and 5). This shows that the W323 residue is already acting to disrupt the base stacking and to destabilize the DNA helix. Furthermore, the enrichment of the slow complex in the W323A background (Figure 6A, lane 4) suggests that this disruption is accompanied by a bend in the DNA at, or near, the position of the first nick. This bend is proposed to be an integral component of the mechanism that disrupts the DNA helix in preparation for the hairpin processing steps.

In complex 2, the W298 stacking residue does not promote base flipping as might be expected. On the contrary, two lines of evidence show that it inhibits base flipping and opposes the force exerted by W323. First, the $KMnO_4$ sensitivity at T2 increases almost 10-fold in the W298A background (Figure 4A, lane 3). This cannot be attributed to the loss of protection afforded by the T2–W298 stacking interaction because the crosslinking experiments show that this is not established until after the first nick. Second, the proposed DNA-bending defect of the W323A mutant is rescued in the W298A background when the fast migration of the uncleaved complex is restored (Figure 6A, lane 5). These two lines of evidence therefore suggest that the absence of the bulky side chain in the W298A mutant allows base flipping to take place one step earlier than normal. The opposing roles of W323 and W298 in the transition between complexes 1 and 2 are indicated by the opposing arrows in the rightmost columns of the model (Figure 7).

Complex 3. The nicked complex represents a major structural transition in the DNA at the transposon end. The increase in IdU crosslinking efficiency indicates that T2 is flipped from the DNA helix and stacked against W298 (Figure 2B and C). There is also an increase in the $KMnO_4$ sensitivity at position $T-1$, indicating further disruption of the DNA helix extending in the 5'-direction from the flipped base (Figure 4A, lanes 7 and 9).

Our model proposes that this structural transition is a direct result of the first nick, which increases the flexibility of the DNA and releases the tension present in complex 2. Thus, the nick allows the force exerted by W323 to overcome the resistance offered by W298. This is supported by the rescue of the W323A fast complex

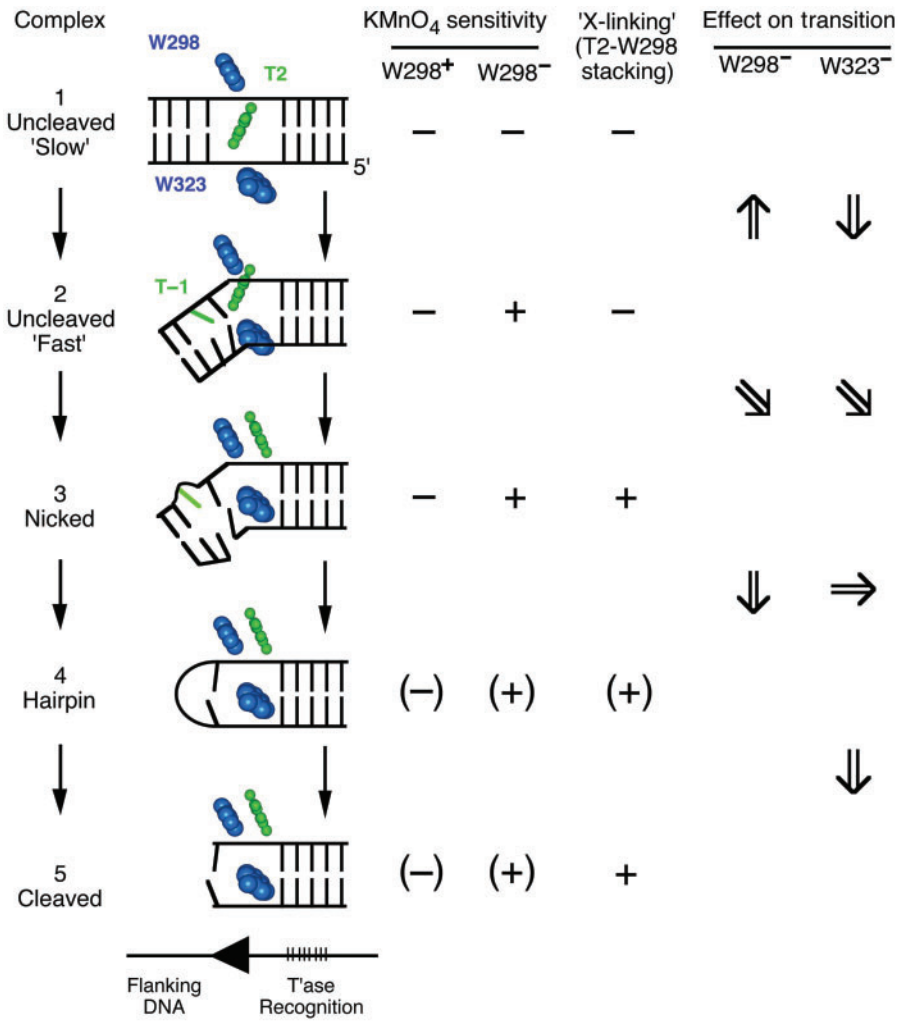

Figure 7. A model for Tn*5* base-flipping dynamics. The model illustrates the base-flipping dynamics during the cleavage step of the transposition reaction. Full details are given in the text. Briefly: In complex 1, the DNA is largely undistorted and the T2 base is stacked in the helix. For clarity, the base opposite T2 has been omitted from the illustration. In complex 2, the DNA is distorted and the probe residue is pushing T2 from the helix against the resistance of the stacking residue. The resistance need not be due to a direct physical interaction. The model is intended to show only that the resistance is abolished by substitution of the tryptophan with the smaller alanine side chain. The opposing roles of the two tryptophan residues in the transition between complexes 1 and 2 are indicated by the opposing arrows in the rightmost columns (see below). In complex 3, the distortion of the DNA increases as the probe residue enters the helix, extruding T2, which is stacked against the second tryptophan. In complex 3, the 3D relationship between T2 and the two tryptophans is taken from the cocrystal structure of the post-cleavage intermediate (see Figure 4B). This relationship is maintained throughout the hairpin processing steps. The model proposes that the flipped base serves to position the top strand of DNA following the increase in steric freedom that will accompany disruption of the helix. Below the illustrations, the transposon end is indicated by the black arrowhead. The specific transposase recognition sequence at base pair +6 to 13 is indicated by the vertical tick marks. The arrows in the two leftmost columns indicate the effects of the tryptophan mutations on the progressive transitions. For example, an upward arrow indicates that mutation of the residue promotes the transition: a downward arrow indicates that the mutation inhibits the transition: a horizontal arrow indicates that the mutation has no effect on the transition: a diagonal arrow indicates a mild effect.

by W298A and/or the first nick (Figure 6A, lanes 5, 9 and 10).

Complex 4. The configurations of the tryptophan residues and the T2 base in the hairpinned intermediate have not been addressed directly in this work. Previous work demonstrated the importance of W298 in the transition from the nicked to the hairpinned complex (34). This agrees with the slow kinetics and loss of specificity seen with mutations at the homologous residue (W265) in Tn*10* (26). Furthermore, since T2 and the tryptophan residues appear to have identical configurations in complexes 3 and 5, they are likely to be similar in complex 4. Indeed, T2 almost certainly remains stacked on W298 in the hairpin intermediate because crosslinked complex 3 performs cleavage in the presence of Mg^{++} (not shown).

Complex 5. The cocrystal structure of the cleaved complex provided the standard against which our current experiments were calibrated. The IdU crosslinking confirmed that T2 was stacked against W298 (Figure 2).

The role of W298 in hairpin resolution has not yet been addressed directly, partly because of the strong defect

at the hairpin-formation step. However, mutations in the homologous W265 residue in Tn*10* delay hairpin resolution and cause it to occur at an imprecise location (26). We have shown that the W323 residue is very important during hairpin resolution (Figure 5A and B). This was unexpected because it is not required during the previous step when the hairpin intermediate is created. One explanation is that its function becomes more crucial following release of the flanking DNA when the destabilizing forces exerted by the DNA bend are necessarily lost.

The role of the T2–W298 stacking interaction

Two general mechanisms have been proposed for base flipping, either passive or active. In a passive mechanism, the T2–W298 stacking interaction would serve to 'capture' a spontaneously flipped base. However, it is now widely acknowledged that base flipping is usually an active process, driven by DNA bending and/or the intrusion of a probe residue. The current results support this view and suggest that base flipping in Tn*5* is driven by the intrusion of the W323 residue, and other factors such as DNA bending. These forces disrupt the DNA helix and provide sufficient steric freedom for processing the hairpin intermediate. What then is the role of the T2–W298 stacking interaction, and why is it required for hairpin formation in Tn*5*? The phenotype of mutations at the homologous W265 residue of the related Tn*10* transposase provides a clue. These mutations form an imprecise hairpin when the 3'-OH at the transposon end attacks the wrong phosphodiester bond (26). We would therefore like to propose that the T2 stacking interactions are used to hold the melted top strand of the DNA in position in the active site for attack by the 3'-OH during the hairpin formation step.

Common elements in different base-flipping reactions

A general model has been proposed for base-flipping reactions (35). Protein binding first distorts the phosphodiester backbone to provide an exit route for the target base out of the helix. A probe residue(s) is then used to push the base out of the helix and/or fill the space vacated. Finally, the flipped base is trapped in an extra-helical location by stabilizing interactions with the protein. Despite substantial variation among the base-flipping structures subsequently reported, this model remains largely valid today. Even so, the Tn*5* base-flipping model presented here unites a surprisingly large number of features observed in other diverse systems.

In Tn*5* complex 1, the principle contacts are between transposase and the specific recognition sequence within the transposon end, 3' to the target base (Figure 7). The DNA bend introduced in the transition between complexes 1 and 2 is promoted by divalent metal ions and presumably requires a change in the transposase contacts in the flanking DNA, 5' to the flipped base. Although the forces that drive base flipping are established during this transition, the T2 base is denied access to stabilization pocket. This series of events is remarkably similar to those proposed for the human 8-oxoguanine glycosylases 1 (hOGG1) (7). In this model, the 3'-interactions are established early, before the 5'-interactions and extrusion of the base. If the base is undamaged, it is denied access to the lesion recognition pocket. However, if the base is 8-oxoG it enters and becomes trapped in the lesion recognition pocket. This is associated with full engagements of the 5'-interactions and the Ca^{++}-dependent stabilization of a sharp bend in the DNA.

Circular permutation and bend-phasing assays suggested that Tn*5* has a sharp bend centered on bp + 2 (33). Although DNA bending is not a universal feature of base-flipping enzymes, the common feature in those systems where it occurs is that the bend is centered on the target base.

The second structural transition in Tn*5* is following the first nick when the probe residue enters the helix and T2 gains access to the stabilization pocket (Figure 7, complex 3). This is associated with further distortion of the DNA extending several nucleotides 5' to the flipped base. This may be a general feature of the mechanism as strand separation in the 5'-direction is also observed in the structures of uracil DNA glycosylases (UDG) and the HhaI methylase (M.HhaI) (3,36,37).

The stacking of T2 against W298 and the insertion of the W323 probe residue in complex 3 locks the components into a stable configuration that persists throughout the subsequent steps. A similar 'lock down' step has been detected in the UDG and M.HhaI reactions.

A ^{19}F-cytosine NMR study of the M.HhaI reaction revealed three distinct transitions referred to as binding, flipping and locking (36). Binding is followed by base flipping, which yields a stable complex in which the target base is extruded from the helix and exists in a heterogeneous conformation. Addition of the AdoMet cofactor induces the final locking step in which the flipped base is immobilized by contacts with the protein. These three stages appear to correspond to the Tn*5* complexes 1, 2 and 3, respectively. The mechanistic implication is that base flipping does not depend on the capture of the base in the stabilization pocket. The subsequent capture of the flipped base in a single conformation is a secondary process arising from some contingency later in the reaction. In the case of M.HhaI, this is holding the base in place for the methylation reaction. For Tn*5*, we suggest in our model that the flipped base is used to hold the melted top strand of the DNA in position for the nucleophilic attack that will generate the hairpin intermediate.

Kinetic analysis of fluorescent changes in UDG suggested a similar stepwise base-flipping mechanism. A rapid base-flipping step, to form an unstable extra-helical intermediate, is followed by an isomerization to establish specific interactions between the enzyme and the flipped uracil base (6,38).

A presteady-state analysis of UDG further suggested that the probe residue does not push the extruded base, but acts as a 'doorstop' to prevent its return (39). Although the W323 probe residue in Tn*5* contributes to base extrusion, it also acts as a doorstop. This is evident from its importance during the hairpin resolution step in the transition between complexes 4 and 5 (Figure 7).

Presumably, it is required to prevent the return of T2 and/or to maintain the proper separation of the DNA strands after the destabilizing influence of the DNA bend is unavoidably lost owing to the double-strand break.

In summary, it appears that base flipping in Tn*5* is driven by a combination of DNA bending and the insertion of a probe residue. Base flipping disrupts stacking within the double helix and provides the steric freedom required for the hairpin processing steps. Stabilizing interactions between the flipped base and the protein hold the second strand in position for cleavage during the hairpin formation step. The probe residue finally performs a second function either to prevent the return of the flipped base or to hold the DNA strand in position for the hairpin resolution step.

MATERIALS AND METHODS

Chemicals and oligonucleotides were from Sigma and BDH Laboratory Supplies. Enzymes were from NEB or Roche Applied Science. Radio-nucleotides were from Amersham Biosciences. All cloned PCR products were confirmed by nucleotide sequencing. All of the mutant Tn*5* transposase derivatives were based on a hyperactive triple mutant which is referred to as 'standard transposase' in the text (see below). All of the transposon ends contained the 19-bp hyperactive 'mosaic' sequence (below). This combination of transposase and transposon end increases the solubility of transposase and the affinity of binding to the transposon end. However, these factors are unlikely to affect the chemical mechanism of the reaction.

DNA substrates for PCR and photo crosslinking

Oligonucleotides were PAGE purified. If required, they were annealed by heating to 96°C for 1 min followed by slowly cooling to room temperature in 10 mM Tris pH 8 and100 mM NaCl. DNA fragments were 5'-end labeled using T4 polynucleotide kinase and [γ-^{32}P]ATP. The sequence of the cleaved substrate top strand was 5′-CTGTCTCTTATACACATCTCGG. The sequence of the uncleaved substrate top strand was 5'-CTGACTGA CTGACTGACAGCTGTCTCTTATACACATCTCGG. The sequence of the respective bottom strand oligonucleotides was the exact complement. The nicked substrate was obtained by annealing the uncleaved substrate top strand with a pair of complementary oligonucleotides: 5'-CTGT CAGTCAGTCAGTCAG and 5'-CCGAGATGTGTAT AAGAGACAG.

The sequences of IdU substrates were identical except that 5-iodo deoxyuracil was incorporated in place of T2. In the crosslinking experiments with the nicked and the precleaved DNA substrates, there was no 5'-phosphate group at the end of the transposon.

DNA substrates for transposition reactions, $KMnO_4$ assay and EMSA

The 19-bp Tn*5* mosaic transposon end, encoded on a 59-bp double-stranded oligonucleotide 5'-AATTCGTGA GCGTGGGTCTCGCGGTCTGTCTCTTATACACAT CTCAACCATCATCGACA, was cloned into the pDRIVE vector (Qiagen) digested with EcoRI and HinDIII. The sequence incorporates an Nb.BsaI recognition site in the flanking DNA that allows the introduction of a specific nick at the 3'-end of the transposon. This nick generates the natural 5'-phosphate group at the end of the transposon. pRC916 (pJB16) was created by digesting this plasmid with BsaHI and AhdI, followed by end filling and self-ligation to eliminate a second BsaI site present in the plasmid. pRC917 (pJB17) is identical to pRC916 except that the T at position −1 in the flanking DNA is changed to a C.

For the EMSA and $KMnO_4$ experiments, DNA substrates were generated by digesting pRC916 with BamHI and XbaI (32-bp flanking DNA and 58-bp transposon arm). The transposon arm (XbaI site) was 3'-end labeled using the exo$^-$ Klenow fragment and [α-^{32}P] dCTP. The DNA fragments were purified by electrophoresis on a 5% polyacrylamide gel and recovered by the crush and soak method. The pre-nicked substrate was prepared in exactly the same way except that it was first digested with the nicking enzyme Nb.BsaI (the generous gift of S.Y. Xu at NEB) (40). The nicking efficiency was monitored by following the relaxation of the supercoiled pRC916 substrate on a TBE-buffered 1% agarose gel. The DNA fragment for the kinetic analysis (42-bp flanking DNA and 58-bp transposon arm) was prepared by digesting pRC916 with MluI and XbaI, followed by 3'-end labeling at both ends as described above.

Protein expression and purification

The IS*50* transposase ORF was amplified from *E. coli* DS580 genomic DNA and cloned into pUC18. The EK54, MA56 and LP372 hyperactive mutants were added sequentially by site-directed mutagenesis. The ORF was subsequently cloned into the NdeI and SmaI sites of the pTYB2 intein expression vector (NEB) to yield pRC604 (pYHK4). Further rounds of site-directed mutagenesis to introduce the mutations W298A (pRC930 = pJB30), W323A (pRC931 = pJB31) and the double mutant W298A–W323A (pRC932 = pJB32). The transposases were expressed and purified as described previously (17), except that the host strain was BL21 DE3 (Novagen).

PEC assembly and activity assay

Transpososomes were assembled in 20 mM Hepes pH 7.5, 100 mM potassium glutamate and 100 μg/ml tRNA, with 5 nM DNA substrate and 50 nM transposase. The standard reaction buffer contained 5 mM $CaCl_2$ and was supplemented with 5 mM $MgCl_2$ to initiate the transposition reaction. In Figure 6, $CaCl_2$ was omitted from the buffer and replaced with EDTA as indicated. Complexes were allowed to form at room temperature for 15 min and moved to 37°C before the start of the reaction. The EMSA was by TBE-buffered 5% PAGE. Cleavage reactions were stopped with EDTA, ethanol precipitated and analyzed by denaturing 10% PAGE (DNA sequencing gel).

$KMnO_4$ assay

Complexes were assembled in standard reaction buffer and treated with 8 mM $KMnO_4$ for 30 s at room

temperature before quenching with a 'stop solution' that achieved a final concentration of 300 mM NaOAc pH 5.5, 30 mM EDTA, 100 mM DTT and 100 μg/ml glycogen. The DNA was recovered in a pellet by ethanol precipitation. The pellet was dissolved in 100 μl of freshly diluted 1 M piperidine by heating to 90°C for 30 min. Following a second round of ethanol precipitation, the DNA was dissolved in TE buffer plus 7 M urea and analyzed on a 10% polyacrylamide DNA sequencing gel.

$KMnO_4$ reactions in the gel slice were similar. The substrate was generated from pRC917 (above). The gel slices were dialyzed against standard reaction buffer for 1 h, then treated with 40 mM $KMnO_4$ for 1 min. After quenching, the complexes were digested with proteinase K (Roche) and eluted from the gel overnight at 50°C. The DNA was recovered by ethanol precipitation and further treated as described above.

Crosslinking assay

Complexes were assembled as described above. An aliquot of each reaction was analyzed in the EMSA to monitor the efficiency of assembly for the purpose of normalizing the crosslinking signal. Half of the remaining sample was retained as a 'no UV' control, while the other half was exposed for 30 min to a Stratagene 2040EV UV Transilluminator (312 nm) at a distance of 8 cm. The reactions were mixed with Laemmli loading buffer, heated for 10 min at 50°C and analyzed by 10% SDS-PAGE. The gel was dried and recorded by autoradiography.

For peptide sequencing to identify the site of crosslinking, 600 pmol of complexes were exposed to UV. The crosslinking efficiency was estimated at 15–20%, yielding ~100 pmol DNA adducts which were dialysed against 100 mM Tris-HCl pH 8.0, 0.01% SDS for 2 h. Trypsin (25 μg, Roche) was added and the sample was incubated overnight at 37°C. The sample was diluted 5-fold in 25 mM Tris-HCl pH 8 and loaded onto an HR5/5 MonoQ cation exchange column on and AKTA FPLC system. The column was equilibrated in 25 mM Tris-HCl pH 8. The elution gradient was from 50 mM 1 M NaCl in the same buffer at a flow rate of 0.7 ml per min. Elution of the DNA was detected by monitoring the ^{32}P end-label on the DNA. The DNA adducts and free DNA eluted at 60 and 63% of the gradient, respectively. Peak fractions were identified by autoradiography following SDS-PAGE on a 15% Tris-Tricine buffered gel. The DNA adducts were recovered in a pellet by ethanol precipitation and the crosslinked peptides were sequenced by automated Edman degradation and microbore HPLC at the MRC Immunochemistry Unit at the Department of Biochemistry, Oxford.

ACKNOWLEDGEMENTS

We would like to thank Yu-Hoi Kang for the crosslinking experiment that produced one of the peptide sequences and Tony Willis for the peptide sequencing. Sven Sewitz first recognized the importance of W323 and suggested the crosslinking strategy. We would also like to thank Phoebe Rice for valuable comments. This work was funded by grants from The Wellcome Trust. Funding to pay the Open Access publication charge was provided by The Wellcome Trust.

Conflict of interest statement. None declared.

REFERENCES

1. Roberts,R.J. and Cheng,X. (1998) Base flipping. *Annu. Rev. Biochem.*, **67**, 181–198.
2. Roberts,R.J. (1995) On base flipping. *Cell*, **82**, 9–12.
3. Klimasauskas,S., Kumar,S., Roberts,R.J. and Cheng,X. (1994) HhaI methyltransferase flips its target base out of the DNA helix. *Cell*, **76**, 357–369.
4. Vrielink,A., Ruger,W., Driessen,H.P. and Freemont,P.S. (1994) Crystal structure of the DNA modifying enzyme beta-glucosyltransferase in the presence and absence of the substrate uridine diphosphoglucose. *EMBO J.*, **13**, 3413–3422.
5. Hollis,T., Ichikawa,Y. and Ellenberger,T. (2000) DNA bending and a flip-out mechanism for base excision by the helix-hairpin-helix DNA glycosylase, Escherichia coli AlkA. *EMBO J.*, **19**, 758–766.
6. Stivers,J.T. (2004) Site-specific DNA damage recognition by enzyme-induced base flipping. *Prog. Nucleic Acid Res. Mol. Biol.*, **77**, 37–65.
7. Banerjee,A., Yang,W., Karplus,M. and Verdine,G.L. (2005) Structure of a repair enzyme interrogating undamaged DNA elucidates recognition of damaged DNA. *Nature*, **434**, 612–618.
8. Carter,A.P., Clemons,W.M., Brodersen,D.E., Morgan-Warren,R.J., Wimberly,B.T. and Ramakrishnan,V. (2000) Functional insights from the structure of the 30S ribosomal subunit and its interactions with antibiotics. *Nature*, **407**, 340–348.
9. Patel,P.H. and Loeb,L.A. (2001) Getting a grip on how DNA polymerases function. *Nature Struct. Biol.*, **8**, 656–659.
10. Franklin,M.C., Wang,J. and Steitz,T.A. (2001) Structure of the replicating complex of a pol alpha family DNA polymerase. *Cell*, **105**, 657–667.
11. Schroeder,L.A. and deHaseth,P.L. (2005) Mechanistic differences in promoter DNA melting by Thermus aquaticus and Escherichia coli RNA polymerases. *J. Biol. Chem.*, **280**, 17422–17429.
12. Heyduk,E., Kuznedelov,K., Severinov,K. and Heyduk,T. (2006) A consensus adenine at position -11 of the nontemplate strand of bacterial promoter is important for nucleation of promoter melting. *J. Biol. Chem.*, **281**, 12362–12369.
13. Liu,D., Crellin,P. and Chalmers,R. (2005) Cyclic changes in the affinity of protein-DNA interactions drive the progression and regulate the outcome of the Tn10 transposition reaction. *Nucleic Acids Res.*, **33**, 1982–1992.
14. Sewitz,S., Crellin,P. and Chalmers,R. (2003) The positive and negative regulation of Tn10 transposition by IHF is mediated by structurally asymmetric transposon arms. *Nucleic Acids Res.*, **31**, 5868–5876.
15. Chalmers,R., Sewitz,S., Lipkow,K. and Crellin,P. (2000) Complete nucleotide sequence of Tn10. *J. Bacteriol.*, **182**, 2970–2972.
16. Reznikoff,W.S. (2002). In: Craig,N.L., Craigie,R., Gellert,M. and Lambowitz,A.M. (eds), *Mobile DNA II*, American Society for Microbiology, Washington, DC, pp. 403–422.
17. Davies,D.R., Goryshin,I.Y., Reznikoff,W.S. and Rayment,I. (2000) Three-dimensional structure of the Tn5 synaptic complex transposition intermediate. *Science*, **289**, 77–85.
18. Kennedy,A.K., Guhathakurta,A., Kleckner,N. and Haniford,D.B. (1998) Tn10 transposition via a DNA hairpin intermediate. *Cell*, **95**, 125–134.
19. Bhasin,A., Goryshin,I.Y. and Reznikoff,W.S. (1999) Hairpin formation in Tn5 transposition. *J. Biol. Chem.*, **274**, 37021–37029.
20. Zhou,L., Mitra,R., Atkinson,P.W., Hickman,A.B., Dyda,F. and Craig,N.L. (2004) Transposition of hAT elements links transposable elements and V(D)J recombination. *Nature*, **432**, 995–1001.
21. McBlane,J.F., van-Gent,D.C., Ramsden,D.A., Romeo,C., Cuomo,C.A., Gellert,M. and Oettinger,M.A. (1995) Cleavage at a V(D)J recombination signal requires only RAG1 and RAG2 proteins and occurs in two steps. *Cell*, **83**, 387–395.

22. Hickman,A.B., Perez,Z.N., Zhou,L., Musingarimi,P., Ghirlando,R., Hinshaw,J.E., Craig,N.L. and Dyda,F. (2005) Molecular architecture of a eukaryotic DNA transposase. *Nature Struct. Mol. Biol.*, **12**, 715–721.
23. Kapitonov,V.V. and Jurka,J. (2005) RAG1 core and V(D)J recombination signal sequences were derived from Transib transposons. *PLoS Biol.*, **3**, 181.
24. Rubin,C.M. and Schmid,C.W. (1980) Pyrimidine-specific chemical reactions useful for DNA sequencing. *Nucleic Acids Res.*, **8**, 4613–4619.
25. Serva,S., Weinhold,E., Roberts,R.J. and Klimasauskas,S. (1998) Chemical display of thymine residues flipped out by DNA methyltransferases. *Nucleic Acids Res.*, **26**, 3473–3479.
26. Allingham,J.S., Wardle,S.J. and Haniford,D.B. (2001) Determinants for hairpin formation in Tn10 transposition. *EMBO J.*, **20**, 2931–2942.
27. Ason,B. and Reznikoff,W.S. (2002) Mutational analysis of the base flipping event found in Tn5 transposition. *J. Biol. Chem.*, **277**, 11284–11291.
28. Bolland,S. and Kleckner,N. (1995) The two single-strand cleavages at each end of Tn10 occur in a specific order during transposition. *Proc. Natl Acad. Sci. USA*, **92**, 7814–7818.
29. Crellin,P., Sewitz,S. and Chalmers,R. (2004) DNA looping and catalysis; the IHF-folded arm of Tn10 promotes conformational changes and hairpin resolution. *Mol. Cell*, **13**, 537–547.
30. York,D. and Reznikoff,W.S. (1996) Purification and biochemical analyses of a monomeric form of Tn5 transposase. *Nucleic Acids Res.*, **24**, 3790–3796.
31. Sakai,J., Chalmers,R.M. and Kleckner,N. (1995) Identification and characterization of a pre-cleavage synaptic complex that is an early intermediate in Tn10 transposition. *EMBO J.*, **14**, 4374–4383.
32. Sakai,J.S., Kleckner,N., Yang,X. and Guhathakurta,A. (2000) Tn10 transpososome assembly involves a folded intermediate that must be unfolded for target capture and strand transfer. *EMBO J.*, **19**, 776–785.
33. York,D. and Reznikoff,W.S. (1997) DNA binding and phasing analyses of Tn5 transposase and a monomeric variant. *Nucleic Acids Res.*, **25**, 2153–2160.
34. Ason,B. and Reznikoff,W.S. (2002) Mutational analysis of the base flipping event found in Tn5 transposition. *J. Biol. Chem.*, **277**, 11284–11291.
35. Cheng,X. and Blumenthal,R.M. (1996) Finding a basis for flipping bases. *Structure*, **4**, 639–645.
36. Klimasauskas,S., Szyperski,T., Serva,S. and Wuthrich,K. (1998) Dynamic modes of the flipped-out cytosine during HhaI methyltransferase-DNA interactions in solution. *EMBO J.*, **17**, 317–324.
37. Slupphaug,G., Mol,C.D., Kavli,B., Arvai,A.S., Krokan,H.E. and Tainer,J.A. (1996) A nucleotide-flipping mechanism from the structure of human uracil-DNA glycosylase bound to DNA. *Nature*, **384**, 87–92.
38. Stivers,J.T., Pankiewicz,K.W. and Watanabe,K.A. (1999) Kinetic mechanism of damage site recognition and uracil flipping by Escherichia coli uracil DNA glycosylase. *Biochemistry*, **38**, 952–963.
39. Wong,I., Lundquist,A.J., Bernards,A.S. and Mosbaugh,D.W. (2002) Presteady-state analysis of a single catalytic turnover by Escherichia coli uracil-DNA glycosylase reveals a ''pinch-pull-push'' mechanism. *J. Biol. Chem.*, **277**, 19424–19432.
40. Zhu,Z., Samuelson,J.C., Zhou,J., Dore,A. and Xu,S.Y. (2004) Engineering strand-specific DNA nicking enzymes from the type IIS restriction endonucleases BsaI, BsmBI, and BsmAI. *J. Mol. Biol.*, **337**, 573–583.